



Maximal transport in the Lorenz equations



Andre N. Souza^a, Charles R. Doering^{a,b,c,*}

^a Department of Mathematics, University of Michigan, Ann Arbor, MI 48109-1043, USA

^b Department of Physics, University of Michigan, Ann Arbor, MI 48109-1040, USA

^c Center for the Study of Complex Systems, Ann Arbor, MI 48109-1120, USA

ARTICLE INFO

Article history:

Received 19 July 2014

Received in revised form 15 October 2014

Accepted 22 October 2014

Available online 5 December 2014

Communicated by A.P. Fordy

Keywords:

Lorenz equations

Rayleigh–Bénard convection

Heat transport

Turbulence

ABSTRACT

We derive rigorous upper bounds on the transport $\langle XY \rangle$ where $\langle \cdot \rangle$ indicates time average, for solutions of the Lorenz equations without assuming statistical stationarity. The bounds are saturated by nontrivial steady (albeit often unstable) states, and hence they are sharp. Moreover, using an optimal control formulation we prove that no other flow protocol of the same strength, i.e., no other function of time $X(t)$ driving the $Y(t)$ and $Z(t)$ variables while satisfying the basic balance $\langle X^2 \rangle = \langle XY \rangle$, produces higher transport.

© 2014 Elsevier B.V. All rights reserved.

1. Introduction

Few mathematical models have had as profound an influence on the development of nonlinear science over the last half century as the Lorenz equations [1]

$$\dot{X} = -\sigma X + \sigma Y \quad (1)$$

$$\dot{Y} = rX - Y - XZ \quad (2)$$

$$\dot{Z} = XY - bZ. \quad (3)$$

This system arises as a severe modal truncation of Rayleigh's 1916 model of two-dimensional buoyancy-driven flow between parallel isothermal plates with stress-free boundaries [2]. In modern nondimensional variables Rayleigh's model is the Boussinesq approximation to the Navier–Stokes equations,

$$\dot{\omega} + J(\psi, \omega) = \sigma \Delta \omega + \sigma \text{Ra} \theta_x \quad (4)$$

$$\dot{\theta} + J(\psi, \theta) = \Delta \theta + \psi_x \quad (5)$$

where the $J(\alpha, \beta) = \alpha_x \beta_y - \alpha_y \beta_x$, $\omega(x, y, t) = \Delta \psi(x, y, t)$ is the vorticity associated with stream function ψ , and $\theta(x, y, t)$ is the deviation of temperature from the steady linear conduction profile. The boundary conditions are $\psi = \psi_{yy} = \theta = 0$ at $y = 0$ and $y = 1$ with everything L -periodic in x . The dimensionless

parameters of the problem are the Prandtl number σ , the ratio of diffusion of momentum to diffusion of heat in the fluid, and the Rayleigh number Ra , a ratio of the driving due to the temperature-drop-induced buoyancy force to the damping diffusion coefficients. Rayleigh proved that the steady conduction solution $\psi = 0 = \theta$ is linearly unstable to perturbations $\sim e^{ikx} \sin \pi y$ when $\text{Ra} > \text{Ra}_c(k) = (k^2 + \pi^2)^3 / k^2$. The smallest critical Rayleigh number, $\frac{27}{4} \pi^4$, is achieved in domains of width $L = \text{integer} \times 2\sqrt{2}$.

Lorenz's variables are modal amplitudes in the Galerkin truncation approximation

$$\begin{aligned} \psi(x, y, t) &= \frac{\sqrt{2}}{\pi} \left(\frac{k^2 + \pi^2}{k} \right) X(t) \sin kx \sin \pi y \\ \theta(x, y, t) &= \frac{\sqrt{2}}{\pi r} Y(t) \cos kx \sin \pi y - Z(t) \frac{1}{\pi r} \sin 2\pi y \end{aligned} \quad (6)$$

where the 'reduced' Rayleigh number $r = \text{Ra}/\text{Ra}_c$ and the domain-shape parameter $b = \frac{4\pi^2}{k^2 + \pi^2}$. The time variable is also rescaled according to $t \rightarrow (k^2 + \pi^2)t$. Solutions of Rayleigh's continuum model are reasonably well approximated by Lorenz's truncation only near the primary bifurcation, i.e., for $r = \mathcal{O}(1)$, but the differential equations are nevertheless of theoretical (and historical) interest even for $r \gg 1$ due to the appearance of chaos in the solutions.

The bulk heat transport is gauged by the Nusselt number Nu , the ratio of the sum of the total (conductive plus convective) heat flux to the flow-independent conductive flux. The convective heat flux is proportional to the correlation between the vertical velocity ψ_x and the temperature θ , which reduces to $\text{Nu} - 1 = \frac{k^2 + \pi^2}{2\pi^2 r} \langle XY \rangle$

* Corresponding author.

E-mail addresses: sandre@umich.edu (A.N. Souza), doering@umich.edu (C.R. Doering).

for Lorenz’s variables where $\langle \cdot \rangle$ indicates the infinite time average (when the infinite time limit of long-but-finite time averages exist). The Nusselt number is a key indicator of the nonlinear response of the system to the driving whose strength is measured by the Rayleigh number (Ra or r). The classical linear and nonlinear stability results for both Rayleigh’s and Lorenz’s models are that the pure conduction state with $Nu = 1$, respectively $\psi = 0 = \theta$ and $X = Y = Z = 0$, is absolutely stable for $Ra < Ra_c \equiv r < 1$ and linearly unstable for $Ra > Ra_c \equiv r > 1$.

It is of both fundamental theoretical interest and practical importance for applications to know the dependence of Nu on Ra , σ , and L . The high Rayleigh number Nu – Ra relationship characterizing turbulent convective heat transport is of interest for theory and experiment [3] and has remained the focus of mathematical analysis for more than half a century [4–6]. For Rayleigh’s original 1916 model described above, for example, the most recent rigorous result is the upper bound $Nu < .29 Ra^{5/12}$ uniformly in σ and L for $Ra > \frac{27}{4} \pi^4$ [7].

The study of rigorous bounds on Nu for solutions of the Lorenz equations has received less attention with the notable exceptions of Malkus [8], Knobloch [9], and Foias et al. [10] who found that the steady state maximizes transport among statistically steady solutions and for invariant measures, and P  tr  lis and P  tr  lis [11] who proved that $\langle XY \rangle \leq b \frac{(r+\sigma-\sqrt{\sigma})^2}{r+\sigma}$ for any solution. In this letter we present two alternative approaches to establish the improved estimate $\langle XY \rangle \leq b(r-1)$, uniformly in σ for $r > 1$, when the long-time limit exists. In case long-time averages do not converge, our result is that the limit supremum of finite-time averages satisfies the bound. Most significantly this upper bound is sharp: it is saturated by the exact steady solutions $(X_s, Y_s, Z_s) = (\pm\sqrt{b(r-1)}, \pm\sqrt{b(r-1)}, r-1)$.

In the next section we employ the so-called “background” method, originally contrived for estimating bulk averaged transport in solutions of the Navier–Stokes and related equations [5], to prove the new upper bound. The subsequent Section 3 introduces and develops a novel optimal control strategy for upper bound analysis to reproduce the result: we relax the momentum equation (1) and treat $X(t)$ as a control variable constrained only by $\langle X^2 \rangle = Pe^2$ to drive the temperature variables via (2) and (3). We prove in this setting that $\langle XY \rangle \leq rb Pe^2 / (b + Pe^2)$. Then auxiliary relation $Pe^2 = \langle XY \rangle$, from the neglected Eq. (1), can be used to connect the optimal transport with solutions of the Lorenz equations, yielding the same bound as obtained from the background analysis. This shows that no time-dependent stirring protocol, whether it solves the first Lorenz equation (1) or not, transports more than the steady flow. We also show, in a certain precise sense, that the steady stirring strategy is the *unique* maximizer.

2. Background analysis

We are interested in the $r > 1$ parameter regime. It is convenient to rewrite the Lorenz equations as

$$\dot{x} = -\sigma x + \sigma r y \tag{7}$$

$$\dot{y} = x - y - xz \tag{8}$$

$$\dot{z} = xy - bz \tag{9}$$

where $X = x$, $Y = ry$ and $Z = rz$ and the Nusselt number in terms of the correlation of $x(t)$ and $y(t)$ is $Nu = 1 + \frac{k^2 + \pi^2}{2\pi^2} \langle xy \rangle$. (Note: do not confuse these lower case x and y variables with the spatial coordinates in Rayleigh’s model discussed in the introduction.)

It is well known that, after possible initial transients, solutions of the Lorenz equations are uniformly bounded in time [12–17]. For example

$$\begin{aligned} & \frac{1}{2} \frac{d}{dt} \left[\frac{1}{r^2} x^2 + y^2 + \left(z - 1 - \frac{\sigma}{r} \right)^2 \right] \\ &= -\frac{\sigma}{r^2} x^2 - y^2 - bz^2 + b \left(1 + \frac{\sigma}{r} \right) z \end{aligned} \tag{10}$$

so that

$$\begin{aligned} & \overline{\lim}_{t \rightarrow \infty} \left[\frac{1}{r^2} x^2 + y^2 + \left(z - 1 - \frac{\sigma}{r} \right)^2 \right] \\ & \leq \begin{cases} \left(1 + \frac{\sigma}{r} \right)^2 & \text{if } \min\{1, \sigma, \frac{b}{2}\} = \frac{b}{2} \\ \frac{b^2(1+\frac{\sigma}{r})^2}{4(b-1)} & \text{if } \min\{1, \sigma, \frac{b}{2}\} = 1 \\ \frac{b^2(1+\frac{\sigma}{r})^2}{4\sigma(b-\sigma)} & \text{if } \min\{1, \sigma, \frac{b}{2}\} = \sigma. \end{cases} \end{aligned} \tag{11}$$

Thus for differentiable functions $F : R^3 \rightarrow R$, long time averages of time derivatives satisfy

$$\begin{aligned} \langle \dot{F}(x, y, z) \rangle_T & \equiv T^{-1} \int_0^T \left[\frac{d}{dt} F(x(t), y(t), z(t)) \right] dt \\ & = \mathcal{O}(T^{-1}) \quad \text{as } T \rightarrow \infty. \end{aligned} \tag{12}$$

Hence, averaging time derivatives of $\frac{1}{2}x^2$, $\frac{1}{2}(y^2 + z^2)$, and $-z$ we deduce the balances

$$0 = -\langle x^2 \rangle_T + r \langle xy \rangle_T + \mathcal{O}(T^{-1}) \tag{13}$$

$$0 = -\langle y^2 \rangle_T - b \langle z^2 \rangle_T + \langle xy \rangle_T + \mathcal{O}(T^{-1}) \tag{14}$$

$$0 = -\langle xy \rangle_T + b \langle z \rangle_T + \mathcal{O}(T^{-1}). \tag{15}$$

Now write $z(t) = z_0 + \zeta(t)$ where, anticipating the result, we choose the time-independent “background” component $z_0 = \frac{r-1}{r}$. Substituting this into (14) and (15) yields

$$0 = -\langle y^2 \rangle_T - b \langle \zeta^2 \rangle_T - 2bz_0 \langle \zeta \rangle_T - bz_0^2 + \langle xy \rangle_T + \mathcal{O}(T^{-1}) \tag{16}$$

$$0 = bz_0 + b \langle \zeta \rangle_T - \langle xy \rangle_T + \mathcal{O}(T^{-1}). \tag{17}$$

Then the combination (16) + $2z_0 \times$ (17) is

$$0 = -\langle y^2 \rangle_T - b \langle \zeta^2 \rangle_T + bz_0^2 + (1 - 2z_0) \langle xy \rangle_T + \mathcal{O}(T^{-1}) \tag{18}$$

so that, adding zero cleverly disguised as $\frac{1}{r} \times$ (13) + $r \times$ (18) to $(r-1) \langle xy \rangle_T$, we have

$$\begin{aligned} (r-1) \langle xy \rangle_T &= rbz_0^2 - \left\langle \left(\frac{x}{\sqrt{r}} - \sqrt{r}y \right)^2 + rb\zeta^2 \right\rangle_T + \mathcal{O}(T^{-1}) \\ &\leq rbz_0^2 + \mathcal{O}(T^{-1}) = b \frac{(r-1)^2}{r} + \mathcal{O}(T^{-1}). \end{aligned} \tag{19}$$

This, in turn, implies

$$\overline{\lim}_{T \rightarrow \infty} \langle XY \rangle_T = \overline{\lim}_{T \rightarrow \infty} r \langle xy \rangle_T \leq b(r-1) = X_s Y_s. \tag{20}$$

Therefore, when the long time limit exists, $\langle XY \rangle = \lim_{T \rightarrow \infty} \langle XY \rangle_T \leq b(r-1)$ as advertised.

As a corollary it is interesting to note that the proof also shows that any sustained time dependence in the solutions, whether periodic or chaotic, strictly lowers the transport. Indeed, the first Lorenz equation (1) and the penultimate expression in (19) imply

$$\langle XY \rangle_T \leq b(r-1) - \frac{1}{\sigma^2(r-1)} \langle \dot{X}^2 \rangle_T + \mathcal{O}(T^{-1}) \tag{21}$$

so that $\langle XY \rangle$ is *strictly* less than $X_s Y_s$ when $\langle \dot{X}^2 \rangle \neq 0$.

This is illustrated in Fig. 1 where we plot the upper limit realized by the non-trivial steady state solutions along with measure-

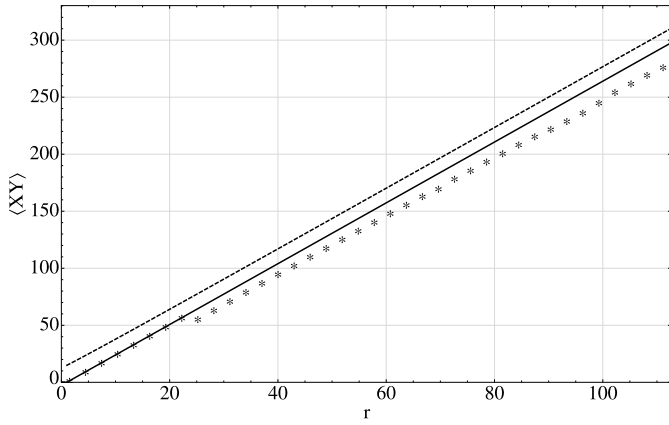


Fig. 1. Long time averaged heat transport for solutions of the Lorenz equations. Dashed line: upper bound on $\langle XY \rangle$ derived by P  tr  lis and P  tr  lis [11]. Solid line: improved upper bound (20) corresponding to the nontrivial fixed points that exist when $r > 1$. Discrete data: direct numerical simulation results for parameter values $\sigma = 10$ and $b = \frac{8}{3}$.

ments of $\langle XY \rangle$ from direct numerical solutions of the Lorenz equations. For these particular parameter values ($\sigma = 10$ and $b = \frac{8}{3}$) the non-zero fixed points are stable for $1 < r \leq \frac{470}{19} = 24.73\dots$ [1] while chaotic and periodic solutions—that necessarily transporting less heat—are robustly realized for higher r .

3. Optimal control analysis

The same upper bound results from an alternative analysis that yields some insight into the dynamics of optimal transport in the Lorenz equations. This approach was recently applied to other Rayleigh–B  nard convection problems with interesting outcomes [18]. The idea is to consider the flow as a control variable driving the temperature field via the advection diffusion equation and ask the following question: What is the maximal transport that can be realized among all flows subject to a suitable intensity constraint? The relevant constraint for Rayleigh’s model is the value of the space–time averaged enstrophy (the mean squared vorticity $\langle \omega^2 \rangle$, where $\langle \cdot \rangle$ includes the spatial average in this context), the magnitude of which becomes a parameter in the control problem. By revisiting the neglected momentum equation we connect the flow intensity parameter with the transport and the original parameter(s): for Rayleigh’s model the connection is established by multiplying (4) by ψ and averaging over space and time to see that $\langle \omega^2 \rangle = \text{Ra} \langle \psi_x \theta \rangle = \text{Ra}(\text{Nu} - 1)$.

For the Lorenz equations we neglect dynamical equation (1) and treat $X(t)$ as a control variable in (2) and (3) for $Y(t)$ and $Z(t)$. The amplitude of X is subject to the constraint $\langle X^2 \rangle = \text{Pe}^2 < \infty$ where the P  clet number Pe parameterizes the strength of the stirring. We seek to determine the optimal $X(t)$ that maximize the convective transport proportional to the correlation $\langle XY \rangle$. Afterwards, to connect the P  clet number to the Rayleigh–B  nard problem, we impose the relation $\text{Pe}^2 = \frac{2\pi^2 r}{k^2 + \pi^2} (\text{Nu} - 1)$ satisfied by natural buoyancy driven flow. The bound on Nu thus obtained, maximizing over a larger class of functions $X(t)$ than just those generated by (1), is also a bound for solutions of the full Lorenz system.

To carry this out it is again convenient to rewrite (2) and (3) as the inhomogeneous and (generally) non-autonomous linear dynamical system

$$\frac{d}{dt} \begin{pmatrix} y \\ z \end{pmatrix} = \begin{pmatrix} -1 & -x \\ x & -b \end{pmatrix} \begin{pmatrix} y \\ z \end{pmatrix} + \begin{pmatrix} x \\ 0 \end{pmatrix} \quad (22)$$

where $y(t) = Y(t)/r$, $z(t) = Z(t)/r$, and $x(t) = X(t)$ is now a locally square integrable function of time subject only to the mean con-

straint $\langle x^2 \rangle = \text{Pe}^2$ (strictly speaking we require $\langle x^2 \rangle_T = \text{Pe}^2 + o(1)$ as $T \rightarrow \infty$). The optimal control problem is a constrained optimization problem: we seek to determine the maximum possible value, over all admissible functions $x(t)$, of the long-time average $\langle xy \rangle$ where $y(t)$ and $z(t)$ solve (22).

According to the calculus of variations the mother functional that we differentiate to derive the Euler–Lagrange equations satisfied by the optimizers is

$$\mathcal{F} = \left\langle xy - \eta(\dot{y} - x + y + xz) + \zeta(\dot{z} - xy + bz) + \frac{\mu}{2}(x^2 - \text{Pe}^2) \right\rangle \quad (23)$$

where $\eta(t)$ and $\zeta(t)$ are Lagrange multipliers enforcing (22) and the real variable μ is the Lagrange multiplier enforcing the intensity constraint. Ignoring initial (and final) conditions for the moment, the Euler–Lagrange equations obtained by setting $\delta\mathcal{F}/\delta y$, $\delta\mathcal{F}/\delta z$, and $\partial\mathcal{F}/\partial\mu$ to zero are, respectively,

$$\frac{d}{dt} \begin{pmatrix} \eta \\ \zeta \end{pmatrix} = \begin{pmatrix} 1 & x \\ -x & b \end{pmatrix} \begin{pmatrix} \eta \\ \zeta \end{pmatrix} - \begin{pmatrix} x \\ 0 \end{pmatrix} \quad (24)$$

and

$$\mu x(t) = y(t)(1 - \zeta(t)) + \eta(t)(1 - z(t)) \quad (25)$$

that prescribes the optimal stirring strategy $x(t)$ in terms of the dynamical variables and the Lagrange multipliers, and the amplitude constraint $\langle x^2 \rangle = \text{Pe}^2$. Note that for a given control $x(t)$ the linear inhomogeneous system (24) for the ‘adjoint’ functions η and ζ is precisely the time reversed dynamics of (22).¹ Operationally one chooses a value of μ , solves the four dimensional nonlinear system consisting of (22) and (24) coupled together by (25), and then evaluates both the sought-after extreme value of $\langle xy \rangle$ the original parameter of the problem, the P  clet number Pe .

The time independent solution of the optimal control problem is

$$x_s = \pm \text{Pe}, \quad y_s = \eta_s = \pm \frac{b \text{Pe}}{\text{Pe}^2 + b}, \quad z_s = \zeta_s = \frac{\text{Pe}^2}{\text{Pe}^2 + b} \quad (26)$$

yielding an extreme transport value

$$x_s y_s = \frac{b \text{Pe}^2}{\text{Pe}^2 + b}. \quad (27)$$

The Lagrange multiplier $\mu = 2b^2/(\text{Pe}^2 + b)^2 \in (0, 2]$ for these solutions. Recalling that the Nusselt number in terms of the correlation of $x(t)$ and $y(t)$ is $\text{Nu} = 1 + \frac{k^2 + \pi^2}{2\pi^2} \langle xy \rangle$ and, from the abandoned ‘momentum’ Lorenz equation (1) the reduced Rayleigh number r is related to Pe and Nu via $\text{Pe}^2 = \frac{2\pi^2 r}{k^2 + \pi^2} (\text{Nu} - 1)$, we may eliminate the P  clet number and express this steady stirring extreme transport

$$x_s y_s = b \left(1 - \frac{1}{r} \right) \iff X_s Y_s = r x_s y_s = b(r - 1), \quad (28)$$

precisely the same transport in fixed-points of the Lorenz equations that we proved in the previous section is an upper bound for all solutions of the Lorenz equations.

In the two following subsections we will first display and discuss some numerically computed time-periodic solutions of the

¹ If we were interested in maximizing the time average of $x(t)y(t)$ over a finite time interval $(0, T)$ given initial conditions $y(0)$ and $z(0)$, the adjoint dynamics in (24) would come equipped with homogeneous final conditions $\eta(T) = 0 = \zeta(T)$, following from the integration by parts involved with evaluating the functional derivatives, suitable to specify the time-reversed evolution.

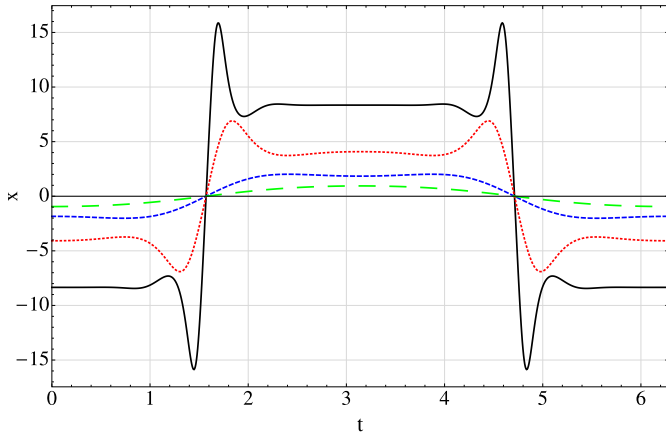


Fig. 2. (Color online.) The time dependence of optimal $\tau = 2\pi$ periodic stirring protocols for several values of the Péclet number and $b = \frac{8}{3}$. Long dashed line: $Pe = 0.69$; short dashed line: $Pe = 1.71$; dotted line $Pe = 4.50$; solid curve: $Pe = 8.96$.

optimal Euler–Lagrange equations, and then prove (a) that the steady solution of the Euler–Lagrange equations realizes the absolute upper bound and (b) that any non-constant time-periodic control transports strictly less. This establishes the fact that steady stirring is the *unique* global maximizer among the infinitely many time-periodic solutions of the Euler–Lagrange equations.

3.1. Time periodic stirring protocols

We numerically constructed some time-periodic solutions of the optimal control problem defined by (22), (24), and (25) by computationally continuing analytical time-periodic solutions from the linearized problem at small Pe into the strongly nonlinear regime. In the limit $Pe \rightarrow 0$ the linearized Euler–Lagrange equations are

$$\dot{y} = -y + x \quad (29)$$

$$\dot{z} = -bz \quad (30)$$

$$\dot{\eta} = \eta - x \quad (31)$$

$$\dot{\zeta} = b\zeta \quad (32)$$

$$\mu x = y + \eta. \quad (33)$$

Let $\tau = \frac{2\pi}{\omega}$ denote the period of the sought-after solutions. Then $z(t) = 0 = \zeta(t)$ and, requiring without loss of generality that $y(t) = \eta(\tau - t)$ to set the phase,

$$y(t) = \frac{\sqrt{2}Pe}{1 + \omega^2}(\cos \omega t + \omega \sin \omega t) \quad (34)$$

$$\eta(t) = \frac{\sqrt{2}Pe}{1 + \omega^2}(\cos \omega t - \omega \sin \omega t) \quad (35)$$

where the Lagrange multiplier $\mu = \frac{2}{1 + \omega^2}$, the optimal control is $x(t) = \sqrt{2}Pe \cos \omega t$, and the transport is $\langle xy \rangle = Pe^2 / (1 + \omega^2)$. To computationally search for τ -periodic solutions of (22), (24), and (25) we first truncate the Fourier series expansion of the full nonlinear system and solve the resulting system of algebraic equations via Newton’s method continuing from small values of Pe using the linearized solutions as the initial guess.

Fig. 2 displays $\tau = 2\pi$ periodic solutions for the control $x(t)$ for several values of the Péclet number. For $Pe > \mathcal{O}(1)$ it is evident that $x(t)$ is ‘attempting’ to take on the steady stirring value $x_s = Pe$ but is frustrated, forced to switch by the mandated periodic behavior.

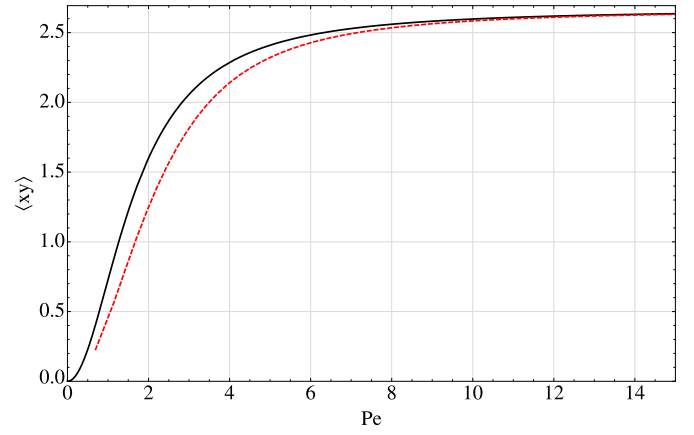


Fig. 3. (Color online.) Solid line: absolute upper bound (53) on the long time averaged transport vs. Péclet number, corresponding to steady stirring, for parameter value $b = \frac{8}{3}$. Dashed line: transport from numerically computed periodic solution of the optimal Euler–Lagrange equations for period $\tau = 2\pi$ ($\omega = 1$), which is observed to lie strictly below absolute upper bound from the steady solutions of the optimal Euler–Lagrange equations.

Fig. 3 is a plot of the absolute upper bound for the transport, $bPe^2 / (b + Pe^2)$, and the transport from numerically computed periodic solutions of the optimal Euler–Lagrange equations for period $\tau = 2\pi$. The time dependent solution produces strictly less transport than steady stirring of the same averaged intensity, as was the case for all periods that we sampled. This suggests that steady stirring is actually the *unique* global optimizer—at least among time-periodic stirring protocols—and in the next subsection we show that this is so.

3.2. Analysis and bounds on transport by arbitrary stirring

Given a general stirring protocol $x(t)$ defined over a semi-infinite interval—without loss of generality $(0, \infty)$ —it is evident that in the long run $y(t)$ and $z(t)$, and hence also the largest possible long time averaged transport $\overline{\lim}_{T \rightarrow \infty} \langle xy \rangle_T$, become independent of the initial data $y(0)$ and $z(0)$. Indeed, if both $y(t)$ and $z(t)$ and $\tilde{y}(t)$ and $\tilde{z}(t)$ satisfy (22) with the same $x(t)$ albeit with different initial conditions, then the differences $\Delta y = y - \tilde{y}$ and $\Delta z = z - \tilde{z}$ satisfy the homogeneous linear system

$$\frac{d}{dt} \begin{pmatrix} \Delta y \\ \Delta z \end{pmatrix} = \begin{pmatrix} -1 & -x \\ x & -b \end{pmatrix} \begin{pmatrix} \Delta y \\ \Delta z \end{pmatrix} \quad (36)$$

so that

$$\frac{d}{dt} \frac{1}{2} ((\Delta y)^2 + (\Delta z)^2) = -(\Delta y)^2 - b(\Delta z)^2 \quad (37)$$

ensuring that the difference $|\Delta y(t)| \leq ce^{-\alpha t}$ for some finite non-negative c depending on $\Delta y(0)$ and $\Delta z(0)$ and $\alpha = \min\{1, b\} > 0$. Then the Cauchy–Schwarz inequality guarantees

$$\begin{aligned} |\langle x \Delta y \rangle_T| &\leq \langle x^2 \rangle_T^{1/2} \left(T^{-1} \int_0^T [\Delta y(t)]^2 dt \right)^{1/2} \\ &\leq (Pe + o(1)) \times \frac{c}{\sqrt{2\alpha T}} \xrightarrow{T \rightarrow \infty} 0. \end{aligned} \quad (38)$$

That being said, we do not know how to solve the Euler–Lagrange equations, or how to prove the existence of solutions in the most general setting. We also do not know that the $T \rightarrow \infty$ limit of $\langle xy \rangle_T$ exists for locally square integrable $x(t)$ for which the $T \rightarrow \infty$ limit of $\langle x^2 \rangle_T$ does exist.

Nevertheless we can be certain that $\langle xy \rangle_T$ is bounded uniformly as $T \rightarrow \infty$ so that the limit supremum is finite and it always

makes sense to seek an upper estimate applicable for all possible values of the long time average. To see this observe that $y(t)$ and $z(t)$ are bounded uniformly in time, independent of the stirring function $x(t)$. Indeed [14],

$$\frac{d}{dt} \frac{1}{2} (y^2 + (z-1)^2) = -y^2 - bz^2 + bz \quad (39)$$

implying

$$\overline{\lim}_{T \rightarrow \infty} [y^2 + (z-1)^2] \leq \begin{cases} 1 & \text{if } 0 < b \leq 2 \\ \frac{b^2}{4(b-1)} & \text{if } b \geq 2. \end{cases} \quad (40)$$

Cauchy–Schwarz thus guarantees

$$\overline{\lim}_{T \rightarrow \infty} \langle xy \rangle_T \leq \text{Pe} \times \begin{cases} 1 & \text{if } 0 < b \leq 2 \\ \frac{b}{2\sqrt{b-1}} & \text{if } b \geq 2. \end{cases} \quad (41)$$

But a much lower *a priori* estimate on the transport, one that is uniform in Pe as $\text{Pe} \rightarrow \infty$, is also easily established:

$$\frac{d}{dt} \frac{1}{2} (y^2 + z^2) = -y^2 - bz^2 + xy \quad (42)$$

so that

$$\langle xy \rangle_T = \langle y^2 + bz^2 \rangle_T + \frac{y(T)^2 + bz(T)^2 - y(0)^2 - bz(0)^2}{2T}. \quad (43)$$

In view of the Pe -independent time asymptotic limits on $|y|$ and $|z|$ in (40), we conclude that $\langle xy \rangle_T$ possesses a Pe -independent upper bound.

To determine the absolute—and, as will be seen, sharp—upper limit start with the differential equation for $z(t)$ in (22) to infer

$$\langle xy \rangle_T = b \langle z \rangle_T + \mathcal{O}(T^{-1}). \quad (44)$$

Then, as in the background analysis, let $z(t) = z_0 + \zeta(t)$, rewrite (43) and $2z_0 \times$ (44) as

$$0 = -\langle y^2 + b\zeta^2 \rangle_T - 2bz_0 \langle \zeta \rangle_T - bz_0^2 + \langle xy \rangle_T + \mathcal{O}(T^{-1}) \quad (45)$$

$$0 = -2z_0 \langle xy \rangle_T + 2bz_0^2 + 2bz_0 \langle \zeta \rangle_T + \mathcal{O}(T^{-1}) \quad (46)$$

and recall that because the infinite time average $\langle x^2 \rangle$ exists,

$$0 = 1 - \frac{1}{\text{Pe}^2} \langle x^2 \rangle_T + o(1). \quad (47)$$

Define

$$a = \frac{b \text{Pe}}{b + \text{Pe}^2} \quad (48)$$

and add 0 in the form of (45) + (46) + $a^2 \times$ (47) to $\langle xy \rangle_T$ to deduce

$$\langle xy \rangle_T = bz_0^2 + a^2 - \left\langle \frac{a^2}{\text{Pe}^2} x^2 + y^2 - 2(1 - z_0)xy + b\zeta^2 \right\rangle_T + o(1). \quad (49)$$

The quadratic form on the right hand side above is non-negative when

$$\frac{a^2}{\text{Pe}^2} - (1 - z_0)^2 \geq 0 \quad (50)$$

which is guaranteed by the choice

$$z_0 = \frac{\text{Pe}^2}{b + \text{Pe}^2}. \quad (51)$$

Then

$$\langle xy \rangle_T \leq bz_0^2 + a^2 + o(1) = \frac{b \text{Pe}^2}{b + \text{Pe}^2} + o(1) \quad (52)$$

and we have proven the global upper bound

$$\overline{\lim}_{T \rightarrow \infty} \langle xy \rangle_T \leq \frac{b \text{Pe}^2}{b + \text{Pe}^2}. \quad (53)$$

Therefore, when the long time limit exists, transport by any protocol $x(t)$ satisfies $\langle xy \rangle \leq b \text{Pe}^2 / (b + \text{Pe}^2)$. This corresponds precisely to the extreme value (27) obtained from the steady solution (26) of the Euler–Lagrange equations for the optimal control problem. Then, utilizing the relation $\text{Pe}^2 = r \langle xy \rangle$ to reintroduce the reduced Rayleigh number r , we conclude that $\langle xy \rangle \leq b(1 - \frac{1}{r})$ even when $x(t)$ does not satisfy the first Lorenz equation.

The analysis above is also sufficient to show that steady control is the unique global optimizer among the class of periodic protocols. To see this, first note that when $x(t) = x_\tau(t)$ is τ -periodic both $y(t)$ and $z(t)$ converge to unique τ -periodic functions $y_\tau(t)$ and $z_\tau(t)$.² This means that the long time average of any continuous function of x , y , and z exists and is equal to the average of the function of $x_\tau(t)$, $y_\tau(t)$, and $z_\tau(t)$ over just one period. In the periodic case (49) with the choice (51) averaged over a period becomes an equality:

$$\langle x_\tau y_\tau \rangle_\tau = \frac{b \text{Pe}^2}{b + \text{Pe}^2} - \left\langle \frac{a}{\text{Pe}} \left(\sqrt{\frac{b}{b + \text{Pe}^2}} x_\tau - \sqrt{\frac{b + \text{Pe}^2}{b}} y_\tau \right)^2 + b \zeta_\tau^2 \right\rangle_\tau. \quad (54)$$

Thus $\langle x_\tau y_\tau \rangle_\tau = \frac{b \text{Pe}^2}{b + \text{Pe}^2}$ if and only if

$$x_\tau(t) = \frac{b + \text{Pe}^2}{b} y_\tau(t) \quad \text{and} \\ \zeta_\tau \equiv 0 \Leftrightarrow z_\tau(t) = z_0 = \text{Pe}^2 / (b + \text{Pe}^2) = \text{constant}. \quad (55)$$

But then the differential equation for $y_\tau(t)$ is

$$\dot{y}_\tau = -y_\tau - x_\tau z_\tau + x_\tau \\ = -y_\tau - \frac{b + \text{Pe}^2}{b} \times y_\tau \times \frac{\text{Pe}^2}{b + \text{Pe}^2} + \frac{b + \text{Pe}^2}{b} y_\tau \equiv 0 \quad (56)$$

so $y_\tau(t) = \text{constant}$ as well. Thus it is proved that the *only* periodic solutions saturating the upper bounds are the constant solutions.

We do not know how to state or prove more general claims about the uniqueness of the steady optimal stirring strategy. One obstruction is the fact that any transiently time-dependent function $x(t)$ that converges to $x_s = \text{Pe}$ as $t \rightarrow \infty$ will produce precisely the same time asymptotic mean transport as $x(t) = x_s$. Moreover, at this stage we do not know how to rule out the existence of optimal protocols that fluctuate non-periodically forever, i.e., $x(t)$ which are not periodic but do *not* converge as $t \rightarrow \infty$, even though the long time average of $\langle x^2 \rangle_T$ does converge to Pe^2 as $T \rightarrow \infty$.

4. Summary and discussion

We have performed two distinct analyses to derive sharp upper bounds on long time averaged transport $\langle XY \rangle_T$ for solutions of the Lorenz equations. The background method was employed to prove that above onset, i.e., for $r > 1$,

$$\overline{\lim}_{T \rightarrow \infty} \langle XY \rangle_T \leq b(r - 1) = X_s Y_s \quad (57)$$

² Indeed, the differences $\Delta y(t) = y(t + \tau) - y(t)$ and $\Delta z(t) = z(t + \tau) - z(t)$ satisfy the homogeneous system (36) when $x(t) = x_\tau(t)$ is τ -periodic, so both $|\Delta y(t)|$ and $|\Delta z(t)|$ converge to zero uniformly (and exponentially) as $t \rightarrow \infty$. This is sufficient to guarantee the existence of a unique periodic solution to the linear inhomogeneous system of differential equations with periodic coefficients defining y_τ and z_τ .

where $X_s = Y_s = \pm\sqrt{b(r-1)}$ along with $Z_s = b - 1$ are the non-trivial fixed points. These steady state solutions will be stable or unstable depending on precise parameter values, but in any case they establish the sharpness of the estimates.

We then adopted an alternative optimal control approach by relaxing the first Lorenz equation (1) while fully enforcing the temperature variable dynamics (2) and (3) to seek the suitably constrained stirring strategy that maximizes transport. The same upper bound emerges from this analysis, a sharp bound saturated by a steady stirring, and we investigated uniqueness of the optimizer by considering time periodic solutions of the Euler–Lagrange equations. We proved that steady stirring is the unique optimizer among appropriately constrained time-periodic controls.

Although the Lorenz equations continue to be the focus of much modern theoretical [19,20], computational [21], and experimental [22] research it is widely appreciated that they do not inform us quantitatively about high Rayleigh number turbulent convection, the problem that provided us with the primary motivation for this investigation. But evaluation of the accuracy of rigorous bounds on heat transport in Rayleigh–Bénard convection remains an important open problem for both physics and mathematics, and studies of simplified systems like this help us to assess the strength of available analytical tools.

Recent application of the optimal control approach developed in Section 3 to spatially extended problems [18] focused on time independent flows. In order to produce bounds that are relevant for turbulent convection, however, optimization must be performed over both steady and non-steady stirring strategies. In this paper we settled the issue for heat transport in the Lorenz equations: steady stirring is the absolute transport maximizer. Not unexpectedly, the question is more complicated in spatially extended systems where the dynamics are defined by nonlinear partial differential equations. Recognizing this, our next step will be to analyze optimal transport in other reduced ordinary differential equation models of Rayleigh–Bénard convection, in particular for certain distinguished higher dimensional Galerkin truncations of Rayleigh's model generalizing the Lorenz equations [23–25].

Acknowledgements

This research was supported by the US National Science Foundation (NSF) Mathematical Physics award PHY-1205219 with an Alliances for Graduate Education and the Professoriate (AGEP) Graduate Research Supplement. The authors also thank S.I. Chernyshenko, G.P. Chini, D. Goluskin, S. Grossmann, P. Hassanzadeh, E. Knobloch, E.A. Spiegel, and J.-L. Thiffeault for helpful discussions. And we gratefully acknowledge the hospitality of Woods Hole Oceanographic Institution's Geophysical Fluid Dynamics Program, supported in part by NSF awards OCE-0824636 and OCE-1332750 and

the Office of Naval Research, where some of this work was completed.

References

- [1] E.N. Lorenz, Deterministic nonperiodic flow, *J. Atmos. Sci.* 20 (1963) 130–141.
- [2] Lord Rayleigh, On convection currents in a horizontal layer of fluid, when the higher temperature is on the under side, *Philos. Mag.* 32 (1916) 529–546.
- [3] G. Ahlers, S. Grossmann, D. Lohse, Heat transfer and large scale dynamics in turbulent Rayleigh–Bénard convection, *Rev. Mod. Phys.* 81 (2009) 503–537.
- [4] L.N. Howard, Heat transport by turbulent convection, *J. Fluid Mech.* 17 (1963) 405–432.
- [5] C.R. Doering, P. Constantin, Variational bounds on energy dissipation in incompressible flows. III. Convection, *Phys. Rev. E* 53 (1996) 5957–5981.
- [6] C.R. Doering, F. Otto, M.G. Reznikoff, Bounds on vertical heat transport for infinite-Prandtl-number Rayleigh–Bénard convection, *J. Fluid Mech.* 560 (2006) 229–241.
- [7] J.P. Whitehead, C.R. Doering, Ultimate state of two-dimensional Rayleigh–Bénard convection between free-slip fixed-temperature boundaries, *Phys. Rev. Lett.* 106 (2011) 244501.
- [8] W.V.R. Malkus, Non-periodic convection at high and low Prandtl number, *Mém. Soc. R. Sci. Liège Ser. 6* (4) (1972) 125–128.
- [9] E. Knobloch, On the statistical dynamics of the Lorenz model, *J. Stat. Phys.* 20 (1979) 695–709.
- [10] C. Foias, M. Jolly, I. Kukavica, E. Titi, The Lorenz equations as a metaphor for the Navier–Stokes equations, *Discrete Contin. Dyn. Syst.* 7 (2001) 403–429.
- [11] F. Pétrélis, N. Pétrélis, Bounds on the dissipation in the Lorenz system, *Phys. Lett. A* 326 (2004) 85–92.
- [12] C.T. Sparrow, *The Lorenz Equations: Bifurcations, Chaos, and Strange Attractors*, Springer Series in Applied Mathematical Sciences, vol. 41, 1982, pp. 1–269.
- [13] V. Reitmann, G.A. Leonov, *Attraktoreingrenzungen für nichtlineare Systeme*, Springer Teubner-Texte zur Mathematik, vol. 97, 1987, pp. 1–196.
- [14] C.R. Doering, J.D. Gibbon, On the shape and dimension of the Lorenz attractor, *Dyn. Stab. Syst.* 10 (1995) 255–268.
- [15] P. Swinnerton-Dyer, Bounds for trajectories of the Lorenz equations: an illustration of how to choose Liapunov functions, *Phys. Lett. A* 281 (2001) 161–167.
- [16] M. Suzuki, N. Sakamoto, T. Yasukochi, A butterfly-shaped localization set for the Lorenz attractor, *Phys. Lett. A* 372 (2008) 2614–2617.
- [17] G. Leonov, A.Y. Pogromsky, K. Starkov, The dimension formula for the Lorenz attractor, *Phys. Lett. A* 375 (2011) 1179–1182.
- [18] P. Hassanzadeh, G.P. Chini, C.R. Doering, Wall to wall optimal transport, *J. Fluid Mech.* 751 (2014) 627–662.
- [19] W. Tucker, A rigorous ODE solver and Smale's 14th problem, *Found. Comput. Math.* 2 (2002) 53–117.
- [20] S. Luzzatto, I. Melbourne, F. Paccaut, The Lorenz attractor is mixing, *Commun. Math. Phys.* 260 (2005) 393–401.
- [21] H.R. Dullin, S. Schmidt, P.H. Richter, S.K. Grossmann, Extended phase diagram of the Lorenz model, *Int. J. Bifurc. Chaos* 17 (2007) 3013–3033.
- [22] L. Illing, R.F. Fordyce, A.M. Saunders, R. Ormond, Experiments with a Malkus–Lorenz water wheel: chaos and synchronization, *Am. J. Phys.* 80 (2012) 192–202.
- [23] Y.M. Treve, O.P. Manley, Energy conserving Galerkin approximations for 2-D hydrodynamic and MHD Bénard convection, *Physica D* 4 (1982) 319–342.
- [24] J.-L. Thiffeault, W. Horton, Energy-conserving truncations for convection with shear flow, *Phys. Fluids* 8 (1996) 1715–1719.
- [25] A. Gluhovsky, C. Tong, T. Agee, Selection of modes in convective low-order models, *J. Atmos. Sci.* 59 (2002) 1383–1393.